MEDICAL DEVICES

An electroadhesive hydrogel interface prolongs porcine gastrointestinal mucosal theranostics

Binbin Ying[1,2,3], Kewang Nan[1,2,4], Qing Zhu[5], Tom Khuu[2], Hana Ro[1], Sophia Qin[3], Shubing Wang[2], Karen Jiang[1], Yonglin Chen[2], Guangyu Bao[6], Josh Jenkins[1,3], Andrew Pettinari[1,3], Johannes Kuosmanen[1,3], Keiko Ishida[2,3], Niora Fabian[1,3,7], Aaron Lopes[1,2,3], Flavia Codreanu[2], Joshua Morimoto[2,3], Jason Li[2,3,8], Alison Hayward[1,2,3,7], Robert Langer[1,3], Giovanni Traverso[1,2,3,8]*

Establishing a robust and intimate mucosal interface that allows medical devices to remain within lumen-confined organs for extended periods has valuable applications, particularly for gastrointestinal theranostics. Here, we report the development of an electroadhesive hydrogel interface for robust and prolonged mucosal retention after electrical activation (e-GLUE). The e-GLUE device is composed of cationic polymers interpenetrated within a tough hydrogel matrix. An e-GLUE electrode design eliminated the need for invasive submucosal placement of ground electrodes for electrical stimulation during endoscopic delivery. With an electrical stimulation treatment of about 1 minute, the cationic polymers diffuse and interact with polyanionic proteins that have a relatively slow cellular turnover rate in the deep mucosal tissue. This mucosal adhesion mechanism increased the adhesion energy of hydrogels on the mucosa by up to 30-fold and enabled in vivo gastric retention of e-GLUE devices in a pig stomach for up to 30 days. The adhesion strength was modulated by polycationic chain length, electrical stimulation time, gel thickness, cross-linking density, voltage amplitude, polycation concentration, and perimeter-to-area ratio of the electrode assembly. In porcine studies, e-GLUE demonstrated rapid mucosal adhesion in the presence of luminal fluid and mucus exposure. In proof-of-concept studies, we demonstrated e-GLUE applications for mucosal hemostasis, sustained local delivery of therapeutics, and intimate biosensing in the gastrointestinal tract, which is an ongoing clinical challenge for commercially available alternatives, such as endoclips and mucoadhesive. The e-GLUE platform could enable theranostic applications across a range of digestive diseases, including recurrent gastrointestinal bleeding and inflammatory bowel disease.

INTRODUCTION

The gastrointestinal (GI) tract presents a challenge for the retention of biomedical materials and devices because of its complex biochemical environment, the rapid turnover of mucus and surface epithelium, and constant motility (*1*–*3*). Current clinical tools like endoclips can be applied rapidly and maintain tissue approximation for weeks to months (*4*, *5*); however, these devices exert mechanical localized force and are unsuitable for scenarios requiring long-term, localized therapeutics or diagnostics that necessitate intimate and stable device-mucosa interaction. Mucosal adhesives, such as hydrogel-based tissue adhesives (*6*–*8*), have been applied in hemostatic sealing (*9*), drug delivery (*10*), and physiological sensing (*11*) in the lumen-confined GI tract. However, existing adhesion mechanisms are generally only retained for ~24 hours. This limitation arises because the physical and chemical bonding sites form primarily in the mucus layers, which are rapidly eliminated through mucociliary clearance within hours (*12*). Mucosal adhesion can be further attenuated by exposure to gastric fluid (*7*). To extend mucosal retention time, adhesives should be able to penetrate the superficial mucosal layers and interact with the deep mucosal epithelium composed of cell types with a much slower turnover rate (*13*); however, mucoadhesive (*14*) and hydrogel tissue adhesives (*6*–*8*) generally have limited ability to penetrate beyond the mucus layer. Alternatively, topological adhesion relies on polymer penetration of the tissue to achieve physical entanglement with the tissue matrix (*15*, *16*); however, such polymers are limited by the slow speed of passive diffusion.

Electrophoretic adhesion, or electroadhesion, occurs when an electric field induces adhesion between nonsticky cationic hydrogels and anionic tissues. A previous study has demonstrated this effect using copolymerized cationic hydrogels and tissues (*17*). However, because the cationic polymers were covalently fixed to the hydrogel backbone, their mobility under electrical stimulation was restrained. Consequently, adhesion occurred only at the surface interface between the tissue and hydrogel (*17*, *18*). Given the rapid turnover of mucus and epithelial cells in mucosal tissues, such surface mucosal adhesion can be limited to fewer than 24 hours (*6*, *7*, *19*).

Here, we report the development of e-GLUE, an electroadhesive hydrogel interface for robust and prolonged mucosal retention. We developed and optimized a tough hydrogel matrix with tissue-like strength, stretchability, and biocompatibility. This hydrogel facilitates the interpenetration of cationic polymers and supports their diffusion into deeper mucosal layers. e-GLUE uses an electrophoretic strategy for mucosal adhesion, enabling material interaction with the deep mucosal epithelium after electrical stimulation. This electrophoretic adhesion extended gastric mucosal retention for up to 30 days. We further demonstrated proof of principle for the potential applications of e-GLUE through in vivo in porcine studies, including the treatment of GI bleeding (*20*), long-term localized therapeutics (*21*),

[1]Department of Mechanical Engineering, Massachusetts Institute of Technology, Cambridge, MA 02139, USA. [2]Division of Gastroenterology, Hepatology and Endoscopy, Brigham and Women's Hospital, Harvard Medical School, Boston, MA 02115, USA. [3]David H. Koch Institute for Integrative Cancer Research, Massachusetts Institute of Technology, Cambridge, MA 02139, USA. [4]College of Pharmaceutical Sciences, Zhejiang University, Hangzhou 310030, China. [5]College of Medical Device, Zhejiang Pharmaceutical University, Ningbo 315104, China. [6]Department of Mechanical Engineering, McGill University, Montreal, QC H3A 0C3, Canada. [7]Division of Comparative Medicine, Massachusetts Institute of Technology, Cambridge, MA 02139, USA. [8]Broad Institute of MIT and Harvard, Cambridge, MA 02142, USA.
*Corresponding author: Email: cgt20@mit.edu

and biosensing devices requiring intimate sensor-mucosa interaction (*22*, *23*).

RESULTS

Optimization of the hydrogel formulation for e-GLUE mucosal adhesion

e-GLUE consists of cationic polymers (polycations) interpenetrated in a tough hydrogel matrix, which can support active polymer diffusion into the deep mucosal layers. With an electrical stimulation treatment of about 1 min, cationic polymers can interact with polyanionic proteins within the deep mucosal tissue (Fig. 1, A and B) that have a relatively slow cellular turnover rate, such as greater than 7 days in the GI tract (*13*). This mechanism increases the adhesion energy between the hydrogel and mucosa by up to 30-fold (Fig. 1, C and D, and movie S1) and extends in vivo retention of e-GLUE devices in porcine stomach for over 30 days through intimate mucosal adhesion (Fig. 1E), which is an ongoing clinical challenge for existing adhesion mechanisms (fig. S1). The rapid and robust adhesion between e-GLUE and the mucosa under electrical stimulation leverages a combination of active polymeric diffusion and polycationic-polyanionic cross-linking (Fig. 1B). To support the adhesion efficacy across different mucosal tissues, we performed electroadhesion across all the segments of the GI tract and observed a significant increase in adhesion strength in all ex vivo porcine tissues tested ($P < 0.05$) (Fig. 1F), despite the presence of intraluminal fluid and mucus layers.

We designed e-GLUE as a tough hydrogel with interpenetrated polycations. We chose to incorporate polycations because of their potential for electrostatic interaction with polyanionic proteins in the mucosal tissues (*24*). A tough hydrogel matrix was chosen to be compatible with polycations; both positive-charged, double-network hydrogels, such as chitosan-polyacrylamide (Chi-PAAm) (*25*), and neutral ones, such as agarose-PAAm hydrogels (*26*), were considered. Unconventional neutral single-network hydrogels, such as highly entangled PAAm (*27*) or poly(ethylene glycol) (PEG) (*28*), were also considered.

We tested six types of polycations: PDAC [poly(diallyldimethylammonium chloride)], P3ATAC {poly[(3-acrylamidopropyl) trimethylammonium chloride]}, P3METAC (poly{[3-(methacryloylamino)propyl]trimethylammonium chloride}), P2ATAC (poly{[2-(acryloyloxy)ethyl]trimethylammonium chloride}), P2DAMA {poly[2-(dimethylamino)ethyl methacrylate]}, and PN3DMA

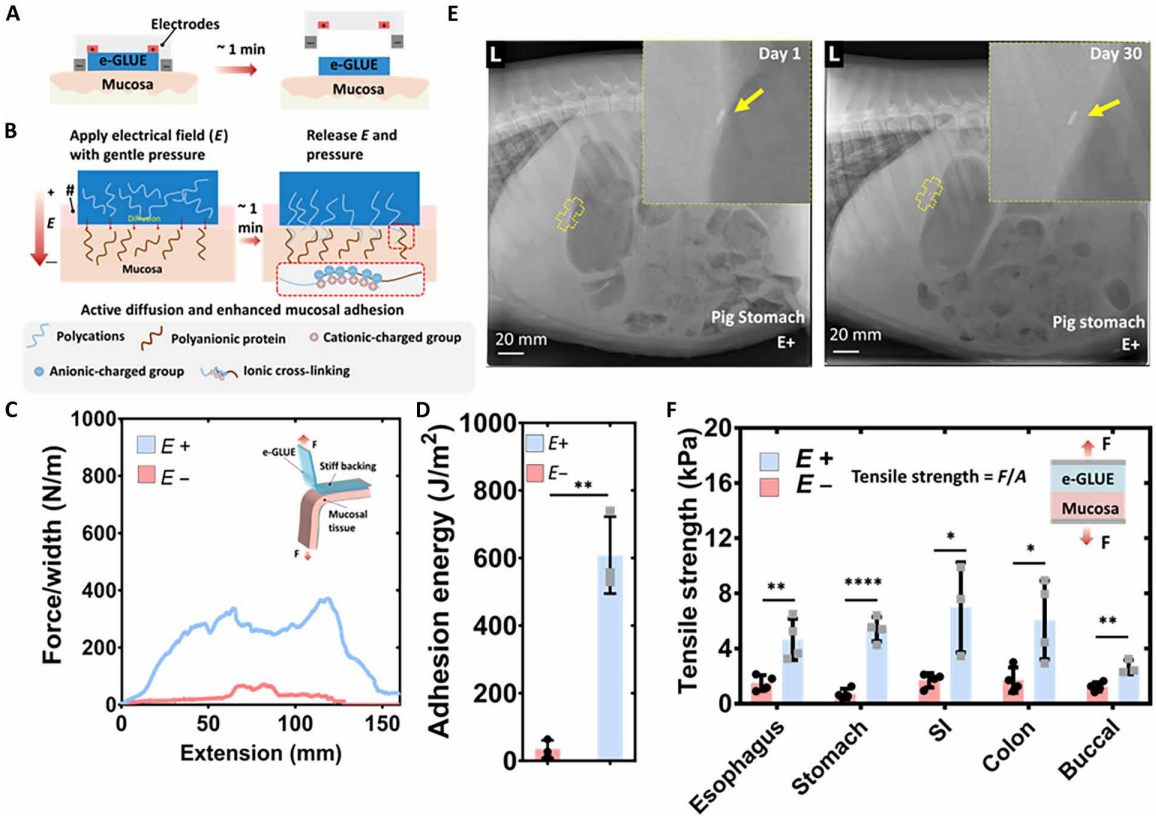

Fig. 1. Electroadhesion interaction between mucosal tissues and e-GLUE. (**A** and **B**) Schematic illustration of e-GLUE deployment with electrodes on the mucosal surface and after removal of the electrode (A) and the electroadhesive mechanism responsible for the strong bonding between e-GLUE and mucosal tissues including a combination of active polymeric diffusion and polycationic-polyanionic cross-linking (B). # in (B) indicates repelled mucus. (**C** and **D**) Representative force-extension curves (C) and adhesion energy difference (D) of e-GULE mucosa hybrids with electrical stimulation treatment (*E*+, blue) or without (*E*−, red) during peeling tests. (**E**) X-ray images showing e-GLUE on the porcine gastric mucosa on day 1 and day 30 after attachment. Yellow arrows show the gastric retention location of e-GLUE labeled with x-ray opaque beads. L indicates the left view of x-ray imaging. Scale bars, 20 mm. $n = 3$. (**F**) Tensile strength of porcine GI mucosal tissues adhered to e-GLUE with (*E*+) and without (*E*−) electrical stimulation (15 V and 40 s). Square-shaped electrodes were used for noninvasive bonding. e-GLUE thickness is 0.75 mm, and polycation concentration is 10%. Data are presented as means ± SD in (D) and (F); dots represent individual replicates. $n = 3$ or 4. Statistical analysis by an unpaired two-sided Student's *t* test. $^*P < 0.05$; $^{**}P < 0.01$; $^{****}P < 0.0001$. Schematic illustrations created with Microsoft PowerPoint.

(poly{*N*-[3-(dimethylamino)propyl]methacrylamide}) (fig. S2), doped in a PAAm single-network hydrogel system to evaluate adhesion properties. We used an alginate-PAAm (Alg-PAAm) hydrogel as a model mucosal tissue in vitro because it closely resembles mucosa in terms of mechanical toughness and polyanionic properties (*29*). After applying a dc electrical stimulation on the preformed e-GLUE mucosa hybrids (fig. S3A), we quantified their adhesion performance using a 180° peel test (Fig. 1C) and tensile tests (fig. S3B). Among the tested polycations, PDAC, P3ATAC, P3METAC, and P2ATAC were measured to have adhesion strengths of ~50 kPa (Fig. 2A), likely because of quaternary amine groups present on these polymers (fig. S2). P2DAMA and PN3DMA had significantly lower adhesion strength compared with PDAC ($P < 0.05$) (Fig. 2A). For subsequent experiments, we doped PDAC (fig. S4A), a commercially available polycation, into a tough hydrogel matrix, such as Chi-PAAm hydrogel, resulting in a PDAC-based e-GLUE capable of stretching over eight times its original length without breaking (fig. S4, B and C). The stretchability of this PDAC-based e-GLUE could potentially withstand displacement in the setting of organ motility (such as GI peristalsis) once the e-GLUE adheres to mucosal surfaces. Compared with neutral hydrogels like agarose-PAAm (*26*), the Chi-PAAm hydrogel matrix was preferred because of its polycationic properties, which further facilitate electroadhesion with tissues (*30*). Furthermore, the ionic interaction between PDAC and Chi-PAAm can effectively minimize excessive diffusion under electrical stimulation, as suggested by previous studies (*31*, *32*). The resulting polymerized e-GLUE device exhibited a Young's modulus of 13.6 kPa (fig. S4C), which is ~50 to 100 times softer than the digestive tract (*33*). To assess the biocompatibility of e-GLUE, we conducted in vitro cytotoxicity tests on cultured mouse embryonic fibroblast cells (NIH/3T3). Fluorescent LIVE/DEAD staining and MTT [3-(4,5-dimethylthiazol-2-yl)-2,5-diphenyltetrazolium bromide] viability assays indicated that 78 ± 2% of the cells remained alive after 24 hours of exposure to the e-GLUE extraction, consistent with cytocompatibility under the International Organization for Standardization (ISO) 10993-5 (fig. S5).

e-GLUE leverages polymer diffusion and ionic cross-linking for enhanced mucosal adhesion

We then investigated the adhesion mechanism between the e-GLUE and the in vitro mucosal tissue model (Alg-PAAm, unless otherwise specified). We hypothesized that the strong bonding between e-GLUE and mucosal tissues that occurs after a short electrical stimulation results from a combination of active polymeric diffusion and polycationic-polyanionic cross-linking (*34*). To visualize the active polymeric diffusion effect, we conjugated fluorescein (fluorescein isothiocyanate) on the polycationic chain [quaternized chitosan, weight-average molecular weight (M_w) = ~90 kDa] in e-GLUE. We observed that the polycations demonstrated minimal mucosal penetration without electrical stimulation (*E*−; fig. S6A). A longer

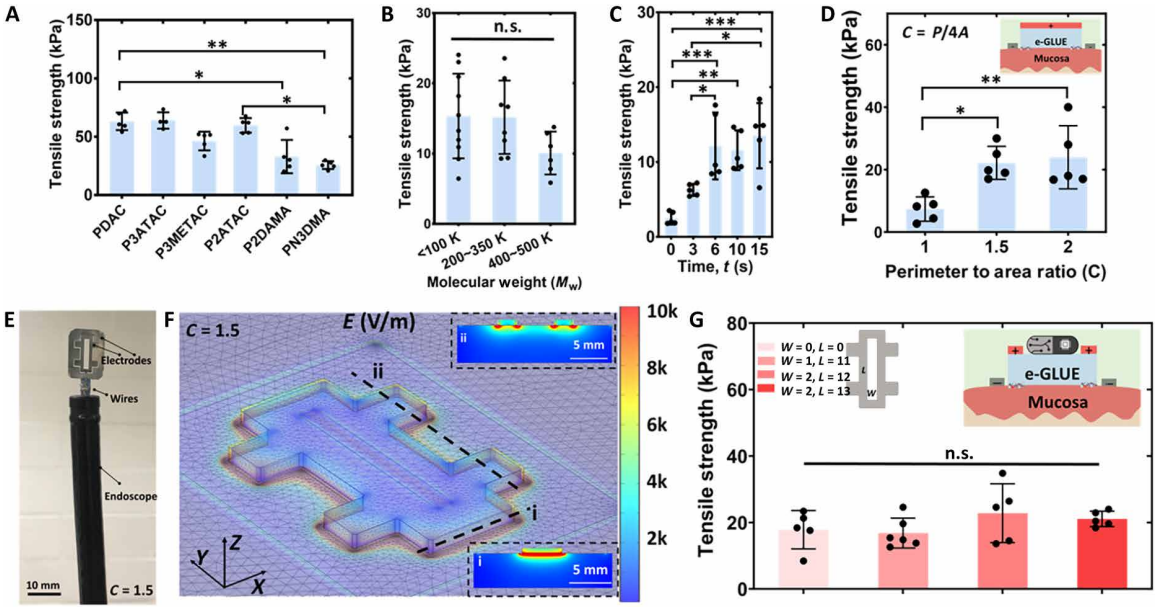

Fig. 2. The adhesion performance of e-GLUE can be tuned by choice of cationic polymer and device dimensions. (**A**) Tensile strength of e-GLUE with different polycations, (**B**) different molecular weights of the cationic polymer chains, or (**C**) the electrical stimulation time. (**D**) Tensile strength of adhesion between mucosa and e-GLUE as a function of the ratio of the electrode perimeter to four times the area. Inset shows the cross-sectional view of noninvasive e-GLUE electrodes. $n = 5$ to 10 replicates. (**E**) Representative photograph of an e-GLUE electrode ($C = 1.5$) inserted into an endoscope for e-GLUE deployment in the GI tract. Rectangular cutout, 2 mm by 12 mm. Scale bar, 10 mm. (**F**) Numerical modeling of the electrical field distribution of the e-GLUE electrode design ($C = 1.5$). The voltage amplitude was set at 10 V. Insets visualize the electrical field distribution of two cross sections. Color scale, 0 to 10,000 V/m. (**G**) Adhesion strength between e-GLUE and porcine duodenal mucosa with different rectangular cutout sizes. The inset schematic proposes a design for a cutout structure in the positive electrode, which can be used to bridge ingestible devices with mucosal tissues through e-GLUE. Data are presented as means ± SD; dots represent individual replicates. $n = 5$ or 6. Statistical analysis in (A) to (D) and (G) by one-way ANOVA and Tukey's multiple comparison test. $^*P < 0.05$; $^{**}P < 0.01$; $^{***}P < 0.001$; n.s., not significant. Schematic illustrations created with Microsoft PowerPoint [(D) and (G)] or COMSOL Multiphysics (F). Conditions used for (A): $d = 0.75$ mm, $U = 15$ V, $t = 40$ s, ρ = 5%, and M_w = ~200 to 350 K; for (B): $d = 0.75$ mm, $U = 6$ V, $t = 10$ s, and ρ = 10%; for (C): $d = 0.75$ mm, $U = 6$ V, ρ = 10%, and M_w = ~200 to 350 K; for (D): $d = 1$ mm, $U = 15$ V, ρ = 10%, $t = 40$ s, and M_w = ~200 to 350 K; and for (G): $d = 0.75$ mm, $U = 15$ V, ρ = 10%, $t = 40$ s, and M_w = ~200 to 350 K.

stimulation time led to a greater polycationic diffusion depth until equilibrium after 60 s (about 80 μm, E+; fig. S6, A and B). This observation is in contrast with the previously reported tissue electroadhesion using cationic hydrogels comprising fully cross-linked networks (*17*), where the achieved adhesion would be localized to the surface and susceptible to rapid mucus and epithelial cell layer turnover (*7*, *19*). To validate polycationic-polyanionic cross-linking, we applied chitosan-free e-GLUE (PDAC-PAAm) to two in vitro models, a mucosal model (Alg-PAAm) and an alginate-free model (PAAm). Upon electrical stimulation, the adhesion force between e-GLUE and Alg-PAAm increased threefold compared with that of e-GLUE and PAAm ($P < 0.01$), indicating the importance of polyanions in the mucosal layer for cross-linking (fig. S6C). Furthermore, the physical entanglement effect between e-GLUE and mucosal layers was negligible given that no significant adhesion enhancement was observed between e-GLUE and PAAm before or after electrical stimulation ($P > 0.05$) (fig. S6D).

We then optimized electroadhesion conditions on the model mucosal tissue by modifying six parameters: e-GLUE polycationic chain length (M_w), electrical stimulation time (t), gel thickness (d), cross-linking density (Cd), voltage amplitude (U), and polycation concentration (ρ). Among the conditions tested, we observed that adhesion performance was negatively correlated with gel thickness (fig. S7A), cross-linking density (fig. S7B), and polycationic chain length (Fig. 2B). Adhesion was positively correlated with voltage amplitude (fig. S7C), stimulation time (Fig. 2C), and polycation concentration (fig. S7D). Reducing thickness below 0.75 mm, increasing voltage amplitude above 6 V, and extending stimulation time beyond 6 s did not result in a significant increase in adhesion performance ($P > 0.05$) (Fig. 2C and fig. S7, A and C). These limits on adhesion performance can be attributed to the saturation of the electrophoresis effect (*35*) resulting from polyion complex formation near the mucosal tissues, which inhibits the further movement of the cationic polymers into the mucosal tissue interior (*34*). Consequently, we selected an e-GLUE with a thickness of 0.75 mm and a PDAC concentration of 10% for subsequent ex vivo and in vivo tests to investigate how the electrode design and stimulation conditions affect mucosal electroadhesion and safety.

The e-GLUE electrode can be adapted for endoscopic-based delivery

To support endoscopic-based translation of e-GLUE, we designed an endoscopically compatible e-GLUE electrode assembly that enabled electrodes to be placed directly on the mucosal surface through minimally invasive surgical techniques (Fig. 2, D and E). We manufactured square-shaped stainless steel electrodes (fig. S7E) through laser cutting and arranged the electrode assemblies to enable noninvasive electrical stimulation by positioning both the positive and negative electrodes on the same side of the tissue. After applying electrical stimulation ($E+$), we measured a significant increase in adhesion strength between the e-GLUE and ex vivo porcine mucosal tissues throughout the GI tract ($P < 0.05$) (Fig. 1F) and other porcine mucosal surfaces in the respiratory, female reproductive, and urinary tracts ($P < 0.01$) ($E+$; fig. S8), in the presence of luminal fluid and mucus layers. In contrast, when electrical stimulation was not applied ($E-$), the adhesion strength between the e-GLUE and tissue was significantly lower ($P < 0.05$) (Fig. 1F and fig. S8). These results suggest that the e-GLUE can support increased adhesion strength of hydrogels to various types of mucosal tissue.

We further optimized the e-GLUE mucosal adhesion strength by adjusting the dimensions of the electrodes, specifically the perimeter (P)–to–area (A) ratio ($C = P/4A$). By increasing C from 1 to 2, the adhesion strength between porcine jejunal mucosa and e-GLUE was significantly increased from 7.4 to 24 kPa ($P < 0.01$) (Fig. 2D). We developed a numerical electromagnetic simulation using COMSOL Multiphysics (version 6.0) to visualize the electrical field distribution with different electrode shapes (Fig. 2F and fig. S9). Numerical results showed that our electrode configuration induced a concentrated electrical field surrounding the area between the positive (located on the e-GLUE) and ground (located on the mucosa) electrodes (fig. S9). A larger C (such as 1.5; Fig. 2E) yielded a longer concentrated electrical field perimeter (Fig. 2F), resulting in a higher adhesion strength (22.2 kPa; Fig. 2D). Increasing C beyond 1.5 did not significantly improve adhesion strength ($P > 0.05$) but involved electrode shape complexity ($C = 2$; Fig. 2D and fig. S7E). In addition, our numerical model predicted that there would be a low electrical field distribution in the central section of the e-GLUE (fig. S9), which is consistent with the low adhesion strength observed during tissue tests (movie S2). We also used the numerical model to optimize electrode design. By reducing the gap between the ground and positive electrodes from 3 to 0.5 mm, the width of the concentrated electrical field expanded from 0.094 mm (gap = 3 mm; fig. S10) to 0.451 mm (gap = 0.5 mm; fig. S10). The numerical model predicted no further increase in the width of the concentrated electrical field, indicating that further gap reduction might not effectively improve the adhesion performance (fig. S10).

To integrate e-GLUE with additional sensors or stimulation electrodes for interfacing with mucosal tissues, we incorporated cutout structures in the positive electrode so that devices can adhere to the bottom of the e-GLUE for prolonged and mucosa localized theranostic applications (inset in Fig. 2G). To study how the cutout geometry affects the adhesion performance, we compared rectangle cutouts with varied widths (W) and lengths (L). Among the tested conditions, the tensile strength between e-GLUE and duodenal mucosa showed no significant difference ($P > 0.05$) (Fig. 2G). Thus, an optimized e-GLUE electrode ($C = 1.5$; gap = 0.5 mm) with cutout structures in the positive electrode (such as 2 mm by 12 mm; Fig. 2E) was selected for subsequent in vivo tests to study how electrical stimulation conditions would affect mucosal electroadhesion and safety.

Safety of e-GLUE and GI retention time in a porcine model

We then assessed the safety and long-term retention efficacy of e-GLUE on the GI mucosa using an in vivo model in swine. Electrical stimulation treatment enables strong bonding between e-GLUE and mucosal tissues but results in increased tissue temperature because of Joule heating. To identify a safe electrical stimulation range, we first used the optimized e-GLUE electrode to investigate how two primary factors, U and t, affect tissue temperature in vivo without sacrificing adhesion performance. On-site tensile tests were performed to quantify the adhesion strength between e-GLUE and live mucosal tissues, such as the small intestine (SI) and stomach. During the stimulation, we used an infrared (IR) camera to monitor the mucosal tissue temperature of an anesthetized swine. Our tests showed that $U = 10$ V and $t = 80$ s yielded an optimal adhesive strength of 16 to 17 kPa with the maximum tissue temperature of 43°C (Fig. 3, A to C). Increasing the stimulation time did not result in a higher adhesive strength (fig. S11), possibly because of the electrophoresis

saturation effect. Increasing voltage reduced the time to achieve a comparable adhesion strength; for example, 10 V and 80 s yielded similar adhesion strength as 20 V and 25 s (Fig. 3A); however, 20 V and 25 s induced a significantly higher temperature ($P < 0.01$) (Fig. 3B) because of a larger corresponding current and Joule heating (fig. S12).

Histological assessment by a board-certified veterinary pathologist blinded to the sample group indicated that, at temperatures under 43°C for 1 min (Fig. 3D), the gastric mucosa exhibited mild inflammation around the e-GLUE perimeter with no visible tissue damage in the middle and deep mucosa (Fig. 3E). In addition, we included a bioheat module into the numerical simulations model to visualize the spatial-temporal temperature distribution of the coupled hydrogel-mucosa structure in the depth direction (Fig. 3F). The simulation predicted that, with electrical stimulation, the surface mucosal tissue along the e-GLUE perimeter would heat to 43°C by 20 s; because of the heat transfer effect, the top 200 μm of mucosal tissue would reach 43°C by 80 s (red zones in Fig. 3F and movie S3). This numerical simulation is consistent with the histological assessment and temperature readings (Fig. 3, D and E), supporting the thermal safety of the e-GLUE technology (*36*). The temperature increase can be further mitigated by applying pulse waveforms (fig. S13A) to dissipate heat without sacrificing adhesion strength (fig. S13B). Therefore, subsequent adhesion experiments used $U = 10$ V and $t = 80$ s for in vivo tests unless otherwise stated.

Achieving long-term retention within the dynamic and active GI luminal environment poses a considerable challenge. To assess the long-term retention of e-GLUE on the GI mucosa, we conducted endoscopic deployment by inserting the electrodes and e-GLUE through the esophagus into the stomach of swine ($n = 3$ animals; one device each) (Fig. 4A, fig. S14, and movie S4) and through the rectum into the colon of swine ($n = 3$; one device in pig one and two devices in pig two). To visualize the gastric retention time, we embedded x-ray opaque stainless steel rods into the e-GLUE. During the in vivo experiments, the gentle pressure from the endoscope ensured firm contact between the devices and the tissue in the dynamic GI environment (movie S3). After electrical stimulation, the electrodes, along with the endoscope, were retrieved from the GI tract (Fig. 4A and fig. S14). X-ray imaging revealed that the e-GLUE retention time on the gastric mucosa ranged from 11 to at least 30 days (Figs. 1E and 4B). On the colon mucosa, e-GLUE remained for over 4 days but no longer than 8 days (Fig. 4B), as determined by the time of the last endoscopic imaging where the e-GLUE was no longer visible. In contrast, hydrogel tissue adhesives [Alg-PAAm with 1-ethyl-3-(3-dimethylaminopropyl)carbodiimide (EDC) and *N*-hydroxysuccinimide (NHS)] that adhered to porcine gastric mucosa primarily relied on physical and chemical bonding mechanisms, such as NHS ester (*37*), and were observed to pass through the GI tract within 2 days ($n = 8$ devices; four devices per pig) (Fig. 4B and fig. S15). These results demonstrate the longer gastric retention time

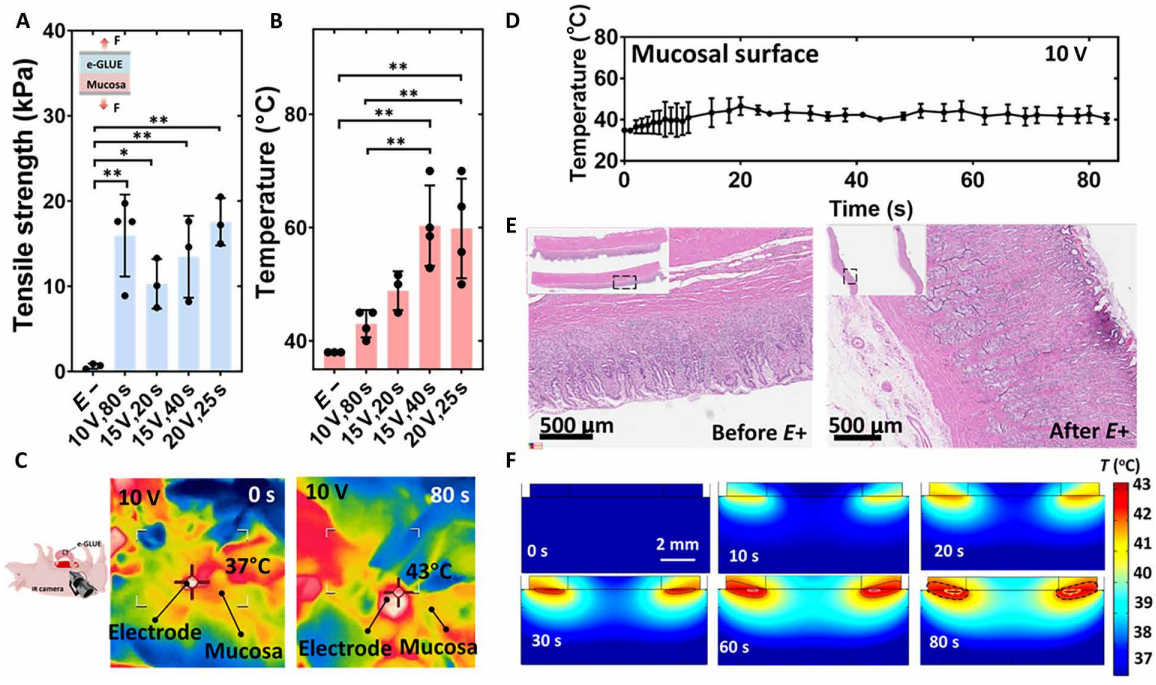

Fig. 3. The tissue temperature can be tuned by the choice of electrical stimulation conditions. (**A**) Adhesion strength of e-GLUE on porcine gastric mucosal tissue in vivo under various electrical stimulation conditions. *E*−, no electrical stimulation. (**B**) Maximum temperature of local porcine gastric tissue under electrical stimulation measured with an external IR camera under anesthesia. (**C**) IR images illustrating temperature distribution on the mucosal tissue before (0 s) and after (80 s) electrical stimulation treatment at a voltage amplitude of 10 V. (**D**) Maximum temperature of local mucosal tissue over 80 s. (**E**) Representative H&E histological images of gastric mucosal tissues before and after 10-V electrical stimulation (*E*+) for 80 s. Inset dashed rectangles, e-GLUE perimeter and enlarged area. Scale bars, 500 μm. (**F**) Three-dimensional electromagnetic-bioheat transfer simulations using COMSOL Multiphysics (version 6.0) to visualize spatial-temporal temperature distribution in the hydrogel-tissue coupling structure in the depth direction over 80 s. Color scale, 37° to 43°C. Voltage amplitude, 10 V. Scale bar, 2 mm. Data presented as means ± SD; dots represent individual replicates in (A), (B), and (D). $n = 3$ or 4 replicates; $N = 2$ pigs were used for these studies. Statistical analysis by one-way ANOVA and Tukey's multiple comparison test. $^*P < 0.05$; $^{**}P < 0.01$. Schematic illustrations created with BioRender (C) or COMSOL Multiphysics (F).

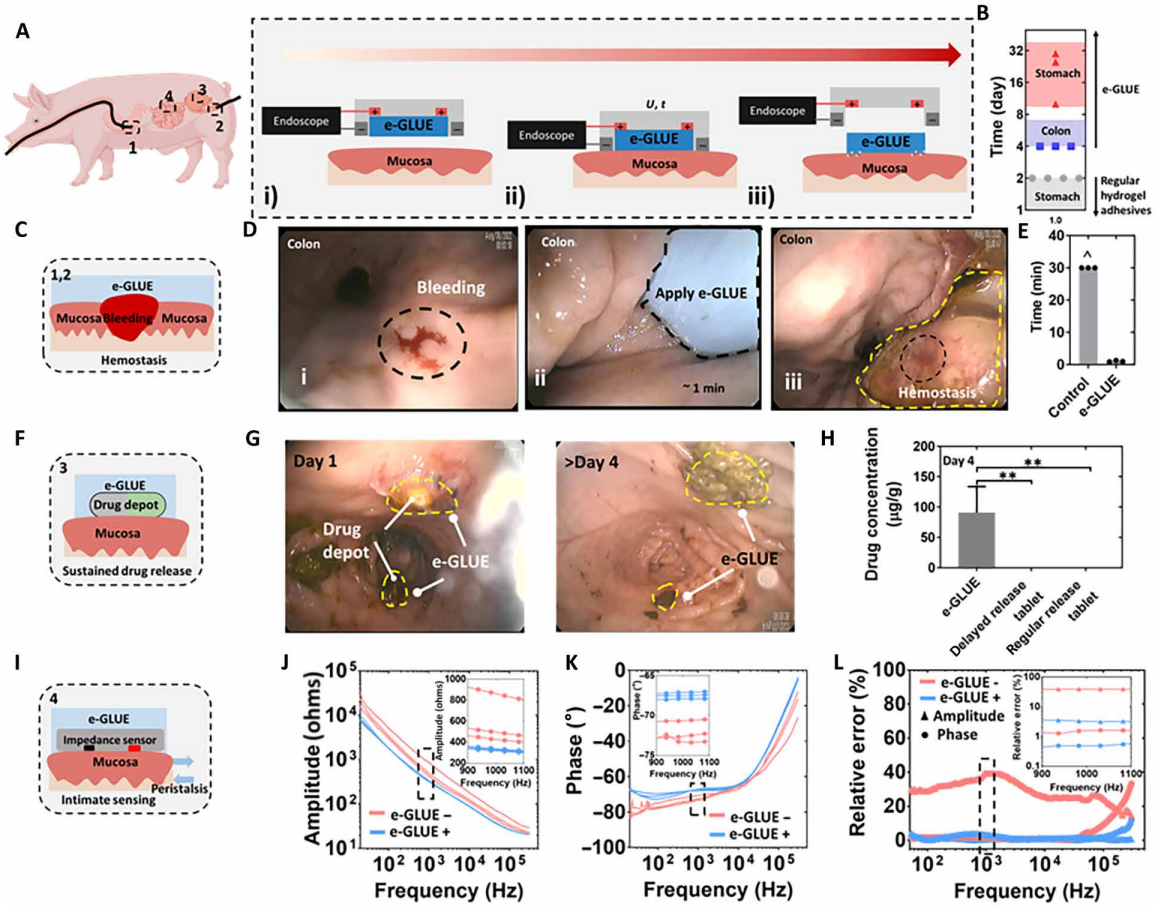

Fig. 4. e-GLUE demonstrated nearly instant mucosal sealing, sustained therapeutic delivery, and intimate biosensing in porcine GI tract models in vivo. (**A**) Schematic illustrating the endoscopic deployment of e-GLUE throughout the entire GI tract for assessment of hemostasis in the stomach and colon (1 and 2), drug deposition in the colon (3), and impedance sensing in the small intestine (4). Schematics show e-GLUE with an attached electrode deployed through an endoscope (i), adhesion triggered with electrical current (ii), and removal of the electrode through the endoscope (iii). (**B**) Retention range of e-GLUE (red, gastric; blue, colon mucosa) and regular hydrogel adhesives (gray for gastric mucosa). Symbols represent the last visualization date under x-ray or endoscope. (**C**) Schematic of e-GLUE applied for mucosal hemostasis. (**D**) Endoscopic view visualizing the hemostasis procedures in the colon, including bleeding (i), application of e-GLUE (ii), and hemostasis (iii). (**E**) Comparison of wound sealing time with and without e-GLUE on the gastric mucosa. ^Untreated wounds on the stomach bled continuously for the entire 30-min monitoring period. $n = 3$ or 4 replicates. (**F**) Schematic of budesonide-loaded e-GLUE adhered to mucosal tissues for prolonged local drug delivery. (**G**) Endoscopic view showing the budesonide-loaded e-GLUE adhered to the colon mucosa at two sites for more than 4 days. (**H**) Budesonide concentration on day 4 in colon tissue through either e-GLUE or oral administration. $n = 3$ or 4 replicates. (**I**) Schematic illustrating the adhesion of an e-GLUE–sensor hybrid on mucosal tissues under peristalsis. (**J**) Amplitude values and (**K**) phase values of three sets of impedance measurements on the same SI mucosal tissue using commercial sensors. (**L**) Calculation of relative errors as the SD divided by the mean value for sensors with e-GLUE (e-GLUE+) and without e-GLUE (e-GLUE–). Data in (E) and (H) are presented as mean and SD. $n = 3$ or 4. Values in (J) and (K) represent three individual tests. Insets in (J) to (L) feature the amplitude, phase, and relative errors around 1 kHz. Statistical analysis in (H) by one-way ANOVA and Tukey's multiple comparison test. $^{**}P < 0.01$. Schematic illustrations created with created with BioRender (A) or Microsoft PowerPoint [(A), (C), (F), and (I)].

of e-GLUE compared with the existing adhesive strategies used on the GI tract (*38*–*40*). We additionally explored the long-term safety of e-GLUE technology by examining mucosal tissues of the proximal duodenum, colon, and stomach at the study termination by hematoxylin and eosin (H&E) staining and pathological evaluation ($n = 3$ pigs; days 24, 30, and 60). No scarring or inflammation was observed, suggesting that the e-GLUE did not cause long-term damage to the GI mucosa in this study (fig. S16).

e-GLUE demonstrated nearly instant mucosal sealing in porcine GI tract models in vivo

With both increased adhesion strength and extended gastric retention validated in vivo, we demonstrated e-GLUE for instant mucosal sealing, sustained local delivery of therapeutics, and intimate biosensing applications in the GI tract. GI bleeding and perforations are clinically life-threatening conditions (*41*). Here, we report the e-GLUE system, which can be used for nearly instant hemostasis and sealing on the GI mucosa (Fig. 4C). To test this capability, we induced bleeding through an acute laceration (5 to 20 mm in length) using a scalpel, endoscopic forceps, or surgical scissors on the GI mucosa, including the colon (Fig. 4D) and stomach (fig. S17), in anesthetized swine ($n = 2$ pigs). Immediate e-GLUE treatment ($d = 22$ mm) was applied on mucosal bleeding sites in the colon for 80 s (Fig. 4D), with effective hemostasis observed ($n = 3$ devices; one device in pig one and two devices in pig two) (Fig. 4, D and E, and fig. S17, A and B). In contrast, untreated wounds were observed

to bleed continuously for the entire 30-min monitoring period ($n = 4$) (Fig. 4E). Although clipping can effectively stop bleeding of small lesions (~5 mm) (fig. S17C), its hemostatic capacity is limited for large bleeding lesions (15 to 20 mm) even when using two clips ($n = 3$) (fig. S17D). Conversely, e-GLUE ($d = 22$ mm) successfully stopped the bleeding after just 80 s of treatment on large bleeding sites ($n = 3$) (fig. S17, A and B). In addition, we observed that removing e-GLUE from the bleeding site resulted in rebleeding ($n = 3$) (fig. S17B), further demonstrating its hemostatic capability for large bleeding lesions. With its prolonged adhesion time, e-GLUE has the potential to address recurrent GI bleeding events (*9*, *42*).

e-GLUE demonstrated sustained, localized therapeutic delivery in porcine GI tract models in vivo

Treatment of inflammatory bowel disease (IBD) can be challenging because of the limited duration of action of orally administrated drugs, which also are associated with systemic side effects (*43*). For example, budesonide is clinically used to treat mild to moderate active IBD, including Crohn's disease and ulcerative colitis. The duration of action for budesonide, however, is limited to 12 hours. Drug depots that can remain resident in the area of the inflammatory mucosal tissue could effectively maximize drug on-target effects while minimizing systemic side effects (*43*). To address this spatial-temporal challenge, we developed an e-GLUE–based drug delivery system that can be attached to specified GI mucosa for sustained therapeutics (Fig. 4F). To demonstrate this, budesonide-loaded PLGA films with a drug mass concentration of 33% as slow-release drug depots were fabricated for in vivo sustained therapeutic purposes because of their high drug payload (fig. S18A) and mechanical flexibility (fig. S18B). After the enema procedure, the PLGA drug film was attached to the colon mucosa with the support of e-GLUE upon electrical stimulation. To mitigate the temperature rise during electrical stimulation, we applied a pulse stimulation with parameters of 15 V and 0.1 Hz in the duty cycle of 15% for 4 min (fig. S13A), providing additional protection to the sensitive colon tissue (movie S5). e-GLUE extended the retention time of drug depots on the colon mucosa for more than 4 days ($n = 3$ devices; one device in pig one and two devices in pig two) (Fig. 4, B and G, and movie S6), despite the rapid epithelium cellular renewal and mechanical shear force stemming from daily bowel movements. The drug concentration in local colon mucosa with e-GLUE treatment was significantly higher than that of orally administered budesonide pills ($P < 0.01$) on days 2 and 4 (Fig. 4H and fig. S18C). Undetectable drug content in the serum over the course of e-GLUE treatment (fig. S18D) indicated negligible systemic drug circulation. No gross tissue damage was observed through endoscopic imaging after 8 days (fig. S18E and movie S7), further supporting e-GLUE compatibility with the GI mucosa and the potential for e-GLUE to be applied for local sustained drug delivery.

e-GLUE demonstrated mucosal biosensing in porcine GI tract models in vivo

Sensors capable of tracking physiologic signals (such as tissue impedance) at defined regions of the GI mucosa can provide valuable health information for conditions such as bowel inflammation (*44*). However, dynamic GI events, such as peristaltic waves, challenge the sensors' ability to maintain stable contact and retention on the mucosa, thereby limiting measurement precision. We hypothesized that e-GLUE, given its strong mucosal adhesion, could enhance sensing precision by facilitating a robust interface between GI mucosa and sensors (Fig. 4I). To support this hypothesis, we first adhered an impedance sensor to intestinal mucosa using e-GLUE during in vivo tests (using one pig) (fig. S19A). e-GLUE improved the contact between the rigid impedance sensor and intestinal mucosa, even during peristaltic activities. This contact improvement resulted in more precise impedance values during multiple tests ($n = 3$, e-GLUE+ in Fig. 4, J and K). For example, compared with sensors without its support, e-GLUE lowered relative errors around 1 kHz (Fig. 4L), a frequency range most relevant to bioelectronic measurements. Specifically, e-GLUE reduced the relative error in both amplitude and phase, from 39.4 to 3.2% and from 1.6 to 0.48%, respectively (zoom-in view in Fig. 4L). This robust mucosal retention enabled impedance sensing on the intestinal mucosa surface for up to 26 hours ex vivo (fig. S19B) and greater than 1 hour in vivo (fig. S19C), where current ingestible solutions cannot achieve such stability. Moreover, the robust mucosal retention of sensors enabled a real-time response of localized GI perturbations, such as temperature changes induced by introduction of hot or cold water (fig. S20). Thus, we determined that e-GLUE–based sensors can respond to localized GI environmental changes through robust sensor-mucosa interfacing. Together with e-GLUE's long-term retention, this system could provide a new paradigm for the localized and chronic monitoring of physiological signals, such as pressure, and biomarkers in defined regions throughout the GI tract.

DISCUSSION

We report the development of e-GLUE, an electroadhesive hydrogel interface that enables robust and long-lasting mucosal retention. e-GLUE electrode design eliminated the need for invasive submucosal placement of ground electrodes for electrical stimulation, addressing a translational challenge that had not been explored in previously reported hydrogel-tissue (*17*) and hydrogel-hydrogel electroadhesion studies (*45*). Potential applications include hemostasis in complex GI environments, long-term localized drug delivery, and intimate biosensing applications throughout the GI tract.

Despite the promising results, this work is limited by the absence of models to fully assess the efficacy of e-GLUE in treating IBD and recurrent GI bleeding in large animal models that are similar to human GI. Future studies should focus on developing and testing e-GLUE in the context of chronic inflammation and recurrent GI bleeding models to more precisely mimic clinical scenarios. In addition, efforts should focus on adapting the e-GLUE device for wirelessly rechargeable sensors, such as impedance and temperature systems, for long-term GI biosensing with untethered real-time data transmission capabilities in pig models. Furthermore, enhancing the antifouling properties of the e-GLUE hydrogel matrix would improve its performance in the complex GI environment.

Overall, this work presents an approach to mucosal adhesion by leveraging electroadhesion and a polycationic tough hydrogel to achieve prolonged retention times on GI mucosa, a critical advancement over existing mucoadhesive technologies (*9*–*11*). Unlike previous methods (*17*, *18*), e-GLUE enables deep interaction with mucosal tissues through active polymer diffusion, extending adhesion in the gastric mucosa from the typical 24-hour limitation to up to 30 days. This finding has key implications for sustained localized drug delivery, improving treatments for GI hemostasis and inflammatory conditions and enhancing other biosensor applications in the dynamic

GI environment where robust mucosal interaction is essential. In addition, our electrode design, which is endoscopically compatible and reduces the need for invasive procedures, further highlights the practical applicability of our approach in real-world clinical scenarios.

MATERIALS AND METHODS

Study design

The objective of this study was to develop an electroadhesive hydrogel interface for intimate and prolonged mucosal retention, enabling mucosal hemostasis, sustained local therapeutic delivery, and biosensing within the GI tract. We hypothesized that this hydrogel could address the retention limitations of existing adhesion mechanisms and commercially available alternatives, such as endoclips. The study investigated the effects of various parameters, such as polycationic chain length, electrical stimulation time, gel thickness, cross-linking density, voltage amplitude, and polycation concentration, on adhesion performance using in vitro mucosal models. The influence of the e-GLUE electrode geometry on adhesion performance was then assessed using ex vivo porcine GI mucosa. Voltage amplitude and stimulation time were evaluated for their effects on adhesion performance and tissue temperature rise using both ex vivo and in vivo porcine GI tissues. Tissue safety was assessed through terminal and survival swine studies, including animal monitoring, histopathological evaluation, and temperature monitoring. Retention longevity was evaluated on gastric and colonic mucosa in survival swine studies. The mucosal sealing performance of e-GLUE was tested in porcine gastric bleeding models and compared with that of commercial endoclips. To validate sustained localized drug delivery, we tested an e-GLUE patch loaded with budesonide-containing PLGA films in swine, measuring tissue and blood pharmacokinetics over 4 days and comparing it with orally administered budesonide pills. Intimate biosensing was assessed using a commercial impedance sensor attached to e-GLUE to monitor porcine intestinal mucosa in vivo for 2 hours and ex vivo for 24 hours. Sample sizes for each experimental group are detailed in the figure legends and were determined on the basis of similar evaluations in the literature. All tests were performed with randomly allocated experimental groups, and no data were excluded from analyses. All animal study protocols were reviewed and approved by the Institutional Animal Care and Use Committee at the Massachusetts Institute of Technology (MIT) (protocol no. 2207000395).

Materials

Ionic cross-linker calcium sulfate ($CaSO_4$; 255548), alginate (A2033), acrylamide (AAm; A8887), covalent cross-linker *N*,*N*′-methylenebis(acrylamide) (MBAA; M7279), free-radical initiator ammonium persulfate (APS; A3678), polymerization accelerator tetramethylethylenediamine (TEMED; T7024), photoinitiator IRGACURE 2959 (I2959), acetic acid (695092), bridging polymer chitosan of medium molecular (448877), the coupling reagents EDC hydrochloride (E1769) and *N*-hydroxysulfosuccinimide (sulfo-NHS, 56485), PDAC solution (409022), and sodium tripolyphosphate (TPP; 238503) were purchased from Sigma-Aldrich. Chitosan (98.2%) was purchased from ChitoLytic. For all ex vivo studies, gastric tissues were collected from either a local farm or within 10 min after euthanasia from a terminal experiment conducted in our lab's animal facility. The tissues were then maintained in Krebs buffer and stored in a 4°C fridge during use.

Fabrication of e-GLUE

The synthesis of e-GLUE was prepared as follows. Briefly, chitosan powder and AAm were first dissolved in acetic acid solution (pH = about 5) at 2 and 12 wt %, respectively, and were stirred overnight until a clean solution was obtained. After degassing, 5 ml of the precursor solution was mixed with 36 μl of 2 wt % MBAA and 8 μl of TEMED in one syringe (BD, 10 ml). Five milliliters of 20 wt % PDAC, 226 μl of 0.27 M APS, and 52.5 μl of 0.75 M TPP were injected into another syringe (BD, 10 ml). All bubbles were removed before further cross-linking. After connecting using a female luer–female luer adapter (Cole-Parmer), the solutions in the two syringes were mixed by pushing the syringe pistons forward and backward 30 times. The mixture was stored inside a closed glass mold at room temperature overnight to allow complete polymerization. Single-network e-GLUE was prepared without chitosan.

Fabrications of alginate-PAAm tough hydrogel

The synthesis of alginate-PAAm tough hydrogel was prepared following a modified protocol based on a previous report (*46*). Briefly, sodium alginate powder and AAm were first dissolved in distilled water at 2 and 12 wt %, respectively, and stirred overnight until a clean solution was obtained. After degassing, 10 ml of the precursor solution was mixed with 36 μl of 2 wt % MBAA and 8 μl of TEMED in one syringe (BD, 20 ml). A 226-μl solution of 0.27 M APS and 191 μl of 0.75 M $CaSO_4$ slurries were injected into another syringe (BD, 20 ml). All bubbles were removed before further cross-linking. After connecting using a female luer–female luer adapter (Cole-Parmer), solutions in two syringes were mixed by pushing the syringe pistons forward and backward 10 times. The mixture was stored inside a closed glass mold at room temperature overnight to allow complete polymerization.

Fabrication of regular hydrogel tissue adhesives

The synthesis of hydrogel tissue adhesives was prepared following a modified protocol based on a previous report (*37*). Briefly, the alginate-PAAm tough hydrogel surface was treated with a mixture of a bridge polymer and coupling reagents for the carbodiimide coupling reaction. The bridge polymer chitosan was dissolved into distilled water at 2.0 wt %, and the pH was adjusted to ~5.5 to 6 by acetic acid. EDC and NHS were used as the coupling reagents. The final concentrations of EDC and NHS in the solution of the bridging polymer were both 12 mg/ml. During GI mucosa bonding, the entire device was pressed on the mucosa for minutes using an endoscope to guarantee a sufficient reaction.

Polymerization of cations

Cations (3ATAC, 3METAC, 2ATAC, 2DAMA, and N3DMA) were dissolved into deionized water in a concentration of 10 wt %. After adding I2959 (0.1%), the cations solutions were exposed to ultraviolet (256 nm) for 1 hour to allow a complete polymerization.

e-GLUE electrode assembly fabrication

e-GLUE electrode assemblies were manually manufactured by assembling four layers, a negative electrode, VHB foam, a positive electrode, and polyethylene terephthalate (PET) film. All features were designed in Solidworks (Dassault Systèmes) and cut using a laser cutting machine (MIYACHI, WL-100A). Copper wires were connected to electrodes with epoxy seal to avoid shorting issues. Rigid heat shrink sleeving was used to encapsulate the copper wires

to guide through the endoscopic channel. The various electrode shapes and dimensions tested are reported in the figures or results.

Strength measurement of e-GLUE

Rectangular strips of e-GLUE (80 mm by 25 mm by 4 mm) were glued to two rigid acrylate clamps (80 mm by 10 mm by 1.5 mm). Samples were prepared for pure shear tests with a universal testing machine (Instron, Model 5543; the loading cell is 250 N). The tensile strain rate was fixed at 200% min^{-1}. The tensile strain (ε) was defined as the length change (Δl) divided by the original length (l_0) of the sample. Young's modulus was calculated from the linear region of the strain-stress curve.

Adhesion performance measurement

Adhesion performance was measured with either 180° peeling or tensile tests. For the 180° peeling test, under electrical stimulation, a ribbon of the e-GLUE (80 mm by 15 mm by 1.4 mm) was adhered to a mucosa mimic gel (Alg-PAAm hydrogel) with one end open, forming a bilayer with an edge crack. The surfaces of e-GLUE and mucosa mimic gel were bonded to a rigid PET film with super glue, to limit deformation to the crack tip. The free ends of e-GLUE and gel were attached to plastic sheets, to which the machine grips were attached. The loading rate was set constant at 100 mm min^{-1}. Adhesion energy, namely, the energy required to increase a unit area of the e-GLUE–substrate interfacial crack was two times the plateau value of the ratio of the force and width. Both force and displacement were recorded continuously throughout the experiment. A minimum of three specimens were used for all mechanical test conditions. For the tensile test, because of the unique configuration of the e-GLUE–mucosa bilayer structure during noninvasive adhesion, a manual mechanical testing stage (Mark-10, model ES20) coupled with a force gauge (Mark-10, model M4-05) was used to apply a precisely controlled tensile pulling force on e-GLUE, which was then converted to adhesive strength using the contacting area.

In vivo experiments

All animal experiments were conducted after the approval the experimental protocols (2207000395) by the Committee on Animal Care at MIT. Swine models were chosen because of their anatomical similarity to humans in GI-related studies (*47*). Randomization of the animals was performed. Female Yorkshire swine (Cummings Veterinary School, Tufts University in Grafton, MA) weighing 43 to 90 kg and aged 3 to 6 months were used. The swine were placed on a liquid diet 24 hours before the study and fasted on the day of the procedure. On the morning of the procedure, the swine were sedated using intramuscular injection of either telazol (5 mg kg^{-1}; tiletamine/zolazepam), xylazine (2 mg kg^{-1}) and atropine (0.04 mg kg^{-1}), or midazolam (0.25 mg kg^{-1}) and dexmedetomidine (0.03 mg kg^{-1}). After intubation, anesthesia was maintained with isoflurane (2 to 3% oxygen). Under anesthesia, vital signs were monitored and recorded every 15 min throughout the study. For survival studies, atipamezole (0.1 mg kg^{-1}) was administered, and recovery was monitored closely. For studies on ambulating animals to monitor long-term gastric retention of the e-GLUE, the swine were fed normally and anesthetized one to two times weekly for radiography.

For mucosal hemostasis demonstration, the swine was anesthetized during terminal (nonsurvival) studies. e-GLUE was applied immediately to mucosal bleeding sites in the colon (after enema and bleeding induced by endoscopic forceps) and in the stomach (by laparotomy with bleeding induced by a scalpel or surgical scissors). For drug delivery demonstration, survival studies were conducted, and the swine was fed normally and anesthetized two times weekly for localized biopsy in the colon. All serum samples were combined with acetonitrile in a 1:3 ratio (v/v) and then centrifuged at 1200 rpm at 4°C for 15 min for protein precipitation and extraction. The supernatant of each tube was then loaded into microtubes and processed using high-performance liquid chromatography (HPLC) to quantify the drug concentrations. For intimate biosensing demonstration, the swine was anesthetized during terminal studies, and e-GLUE with an impedance sensor was applied to mucosal sites in the SI by laparotomy.

In vivo retention and safety evaluation

e-GLUE devices were endoscopically delivered and attached to the gastric mucosa of a swine using an overtube. After electrical stimulation and adhesion, weekly x-ray radiographs were subsequently performed to determine the residency time of the devices. X-rays were taken until all devices passed. During the device retention, the animals were evaluated clinically with no evidence of any changes in feeding or stooling patterns. In addition, the long-term safety of mucosal tissues, including the duodenum, colon, and stomach, treated by e-GLUE was examined both visually and through histological analysis after 7 to 60 days.

Histology

Histological analysis was performed on GI tissue biopsies to characterize the safety. Biopsies were taken from the e-GLUE–treated mucosa from the stomach, SI, and colon within 10 min after euthanasia from a terminal experiment conducted in our lab's animal facility. The biopsies were fixed in formalin fixative (Sigma-Aldrich) for 72 hours before transfer to 70% ethanol. Tissue samples were then embedded in paraffin, cut into 5-μm-thick tissue sections, stained with H&E, and imaged using an Aperio AT2 slide scanner (Leica Biosystems). These samples were analyzed by a board-certified pathologist.

Synthesis of budesonide-PLGA films as slow-release drug depots

Budesonide-PLGA patches were synthesized by uniform precipitation from organic solvents. A 120-mg solution of budesonide and PLGA (PLGA:budesonide = 1:1, 1:1.5, and 1:2) was dissolved in 5 ml of acetone. The mixture was vortexed and sonicated for 0.5 hour to ensure complete dissolution. Then, the mixture was poured into a rectangle glass mold (25 mm by 20 mm) covered with aluminum foil. After 2 days, the budesonide-PLGA films were taken off the glass mold and cut into 15 mm–by–3 mm patches, which have a thickness of around 200 μm.

In vitro release of the budesonide-PLGA film

The in vitro release of budesonide from the budesonide-PLGA film was performed using a horizontal shaker with a speed of 250 rpm at 37°C (Innova Shaker). Phosphate-buffered saline (PBS) (pH 7.4, ×1, Gibco, Thermo Fisher Scientific) was selected as the in vitro medium for drug release kinetics characterization given the intent to target the rectal mucosa environment where extracellular fluid with a similar pH would be encountered. Each budesonide-PLGA patch was added to 10 ml of PBS with 1% Tween 20. Experiments were performed at 37°C, and 1-ml samples were taken daily up to 14 days

after release. Buffers were refreshed at different time intervals, and the drug content was analyzed using HPLC analysis.

Statistical analysis

Statistical analyses were conducted using GraphPad Prism. A normal distribution was assumed for all parametric tests, although this assumption was not formally verified. For comparisons involving multiple samples, a one-way analysis of variance (ANOVA) followed by Tukey's multiple comparison test was performed, with statistical significance defined as $P < 0.05$. For comparisons between two groups, an unpaired, two-tailed Student's t test was applied, with significance also set at $P < 0.05$. Significance levels are represented in the figures as follows: $*P \leq 0.05$, $**P \leq 0.01$, $***P \leq 0.001$, and $****P \leq 0.0001$. Sample sizes for each analysis are specified in the figure legends. All individual-level data can be found in data file S1.

Supplementary Materials

The PDF file includes:
Materials and Methods
Figs. S1 to S20
Legends for movies S1 to S7
Legend for data file S1

Other Supplementary Material for this manuscript includes the following:
Movies S1 to S7
Data file S1
MDAR Reproducibility Checklist

REFERENCES AND NOTES

1. D. H. Altreuter, A. R. Kirtane, T. Grant, C. Kruger, G. Traverso, A. M. Bellinger, Changing the pill: Developments toward the promise of an ultra-long-acting gastroretentive dosage form. *Expert Opin. Drug Deliv.* **15**, 1189–1198 (2018).
2. A. Y. Abuhelwa, D. B. Williams, R. N. Upton, D. J. R. Foster, Food, gastrointestinal pH, and models of oral drug absorption. *Eur. J. Pharm. Biopharm.* **112**, 234–248 (2017).
3. B. Ying, H. Huang, Y. Su, J. G. Howarth, Z. Gu, K. Nan, Theranostic gastrointestinal residence systems. *Device* **1**, 100053 (2023).
4. ASGE technology committee, M. A. Parsi, A. R. Schulman, H. R. Aslanian, M. S. Bhutani, K. Krishnan, D. R. Lichtenstein, J. Melson, U. Navaneethan, R. Pannala, A. Sethi, G. Trikudanathan, A. J. Trindade, R. R. Watson, J. T. Maple, ASGE Technology Committee Chair, Devices for endoscopic hemostasis of nonvariceal GI bleeding (with videos). *VideoGIE* **4**, 285–299 (2019).
5. P. Rogalski, J. Daniluk, A. Baniukiewicz, E. Wroblewski, A. Dabrowski, Endoscopic management of gastrointestinal perforations, leaks and fistulas. *World J. Gastroenterol.* **21**, 10542–10552 (2015).
6. X. Xu, X. Xia, K. Zhang, A. Rai, Z. Li, P. Zhao, K. Wei, L. Zou, B. Yang, W.-K. Wong, P. W.-Y. Chiu, L. Bian, Bioadhesive hydrogels demonstrating pH-independent and ultrafast gelation promote gastric ulcer healing in pigs. *Sci. Transl. Med.* **12**, eaba8014 (2020).
7. S. J. Wu, H. Yuk, J. Wu, C. S. Nabzdyk, X. Zhao, A multifunctional origami patch for minimally invasive tissue sealing. *Adv. Mater.* **33**, e2007667 (2021).
8. H. Yuk, C. E. Varela, C. S. Nabzdyk, X. Mao, R. F. Padera, E. T. Roche, X. Zhao, Dry double-sided tape for adhesion of wet tissues and devices. *Nature* **575**, 169–174 (2019).
9. S. X. Jiang, D. Chahal, N. Ali-Mohamad, C. Kastrup, F. Donnellan, Hemostatic powders for gastrointestinal bleeding: A review of old, new, and emerging agents in a rapidly advancing field. *Endosc. Int. Open* **10**, E1136–E1146 (2022).
10. J. Li, T. Wang, A. R. Kirtane, Y. Shi, A. Jones, Z. Moussa, A. Lopes, J. Collins, S. M. Tamang, K. Hess, R. Shakur, P. Karandikar, J. S. Lee, H.-W. Huang, A. Hayward, G. Traverso, Gastrointestinal synthetic epithelial linings. *Sci. Transl. Med.* **12**, eabc0441 (2020).
11. C. Wang, Y. Wu, X. Dong, M. Armacki, M. Sitti, In situ sensing physiological properties of biological tissues using wireless miniature soft robots. *Sci. Adv.* **9**, eadg3988 (2023).
12. L. M. Ensign, R. Cone, J. Hanes, Oral drug delivery with polymeric nanoparticles: The gastrointestinal mucus barriers. *Adv. Drug Deliv. Rev.* **64**, 557–570 (2012).
13. R. Sender, R. Milo, The distribution of cellular turnover in the human body. *Nat. Med.* **27**, 45–48 (2021).
14. J. D. Smart, The basics and underlying mechanisms of mucoadhesion. *Adv. Drug Deliv. Rev.* **57**, 1556–1568 (2005).
15. J. Yang, R. Bai, Z. Suo, Topological adhesion of wet materials. *Adv. Mater.* **30**, e1800671 (2018).
16. Z. Yang, G. Bao, S. Jiang, X. Yang, R. Huo, X. Ni, L. Mongeau, R. Long, J. Li, Programming hydrogel adhesion with engineered polymer network topology. *Proc. Natl. Acad. Sci. U.S.A.* **120**, e2307816120 (2023).
17. L. K. Borden, A. Gargava, S. R. Raghavan, Reversible electroadhesion of hydrogels to animal tissues for suture-less repair of cuts or tears. *Nat. Commun.* **12**, 4419 (2021).
18. C. K. Roy, H. L. Guo, T. L. Sun, A. B. Ihsan, T. Kurokawa, M. Takahata, T. Nonoyama, T. Nakajima, J. P. Gong, Self-adjustable adhesion of polyampholyte hydrogels. *Adv. Mater.* **27**, 7344–7348 (2015).
19. D. A. Subramanian, R. Langer, G. Traverso, Mucus interaction to improve gastrointestinal retention and pharmacokinetics of orally administered nano-drug delivery systems. *J. Nanobiotechnology* **20**, 362 (2022).
20. N. Ali-Mohamad, M. F. Cau, V. Zenova, J. R. Baylis, A. Beckett, A. McFadden, F. Donnellan, C. J. Kastrup, Self-propelling thrombin powder enables hemostasis with no observable rebleeding or thrombosis over three days in a porcine model of upper gastrointestinal bleeding. *Gastrointest. Endosc.* **98**, 245–248 (2023).
21. S. Babaee, Y. Shi, S. Abbasalizadeh, S. Tamang, K. Hess, J. E. Collins, K. Ishida, A. Lopes, M. Williams, M. Albaghdadi, A. M. Hayward, G. Traverso, Kirigami-inspired stents for sustained local delivery of therapeutics. *Nat. Mater.* **20**, 1085–1092 (2021).
22. Q. Yang, T. Wei, R. T. Yin, M. Wu, Y. Xu, J. Koo, Y. S. Choi, Z. Xie, S. W. Chen, I. Kandela, S. Yao, Y. Deng, R. Avila, T.-L. Liu, W. Bai, Y. Yang, M. Han, Q. Zhang, C. R. Haney, K. Benjamin Lee, K. Aras, T. Wang, M.-H. Seo, H. Luan, S. M. Lee, A. Brikha, N. Ghoreishi-Haack, L. Tran, I. Stepien, F. Aird, E. A. Waters, X. Yu, A. Banks, G. D. Trachiotis, J. M. Torkelson, Y. Huang, Y. Kozorovitskiy, I. R. Efimov, J. A. Rogers, Photocurable bioresorbable adhesives as functional interfaces between flexible bioelectronic devices and soft biological tissues. *Nat. Mater.* **20**, 1559–1570 (2021).
23. Q. Yang, Z. Hu, J. A. Rogers, Functional hydrogel interface materials for advanced bioelectronic devices. *Acc. Mater. Res.* **2**, 1010–1023 (2021).
24. M. Nishikawa, S. Hasegawa, F. Yamashita, Y. Takakura, M. Hashida, Electrical charge on protein regulates its absorption from the rat small intestine. *Am. J. Physiol. Gastrointest. Liver Physiol.* **282**, G711–G719 (2002).
25. G. Bao, R. Huo, Z. Ma, M. Strong, A. Valiei, S. Jiang, S. Liu, L. Mongeau, J. Li, Ionotronic tough adhesives with intrinsic multifunctionality. *ACS Appl. Mater. Interfaces* **13**, 37849–37861 (2021).
26. B. Ying, Q. Wu, J. Li, X. Liu, An ambient-stable and stretchable ionic skin with multimodal sensation. *Mater. Horiz.* **7**, 477–488 (2020).
27. J. Kim, G. Zhang, M. Shi, Z. Suo, Fracture, fatigue, and friction of polymers in which entanglements greatly outnumber cross-links. *Science* **374**, 212–216 (2021).
28. G. Nian, J. Kim, X. Bao, Z. Suo, Making highly elastic and tough hydrogels from doughs. *Adv. Mater.* **34**, e2206577 (2022).
29. B. Ying, X. Liu, Skin-like hydrogel devices for wearable sensing, soft robotics and beyond. *iScience* **24**, 103174 (2021).
30. L. Zhang, D. Yi, J. Hao, Poly (diallyldimethylammonium) and polyphosphate polyelectrolyte complexes as an all-in-one flame retardant for polypropylene. *Polym. Adv. Technol.* **31**, 260–272 (2020).
31. A. Stellwagen, N. C. Stellwagen, Anomalously slow electrophoretic mobilities of DNA restriction fragments in polyacrylamide gels are not eliminated by increasing the gel pore size. *Biopolymers* **30**, 309–324 (1990).
32. N. C. Stellwagen, E. Stellwagen, Effect of the matrix on DNA electrophoretic mobility. *J. Chromatogr. A* **1216**, 1917–1929 (2009).
33. V. I. Egorov, I. V. Schastlivtsev, E. V. Prut, A. O. Baranov, R. A. Turusov, Mechanical properties of the human gastrointestinal tract. *J. Biomech.* **35**, 1417–1425 (2002).
34. A. Xin, R. Zhang, K. Yu, Q. Wang, Mechanics of electrophoresis-induced reversible hydrogel adhesion. *J. Mech. Phys. Solids* **125**, 1–21 (2019).
35. T.-A. Asoh, W. Kawai, A. Kikuchi, Electrophoretic adhesion of biodegradable hydrogels through the intermediary of oppositely charged polyelectrolytes. *Soft Matter* **8**, 1923–1927 (2012).
36. M. W. Dewhirst, B. L. Viglianti, M. Lora-Michiels, M. Hanson, P. J. Hoopes, Basic principles of thermal dosimetry and thermal thresholds for tissue damage from hyperthermia. *Int. J. Hyperthermia* **19**, 267–294 (2003).
37. J. Li, A. D. Celiz, J. Yang, Q. Yang, I. Wamala, W. Whyte, B. R. Seo, N. V. Vasilyev, J. J. Vlassak, Z. Suo, D. J. Mooney, Tough adhesives for diverse wet surfaces. *Science* **357**, 378–381 (2017).
38. V. Gupta, B.-H. Hwang, N. Doshi, A. Banerjee, A. C. Anselmo, S. Mitragotri, Delivery of exenatide and insulin using mucoadhesive intestinal devices. *Ann. Biomed. Eng.* **44**, 1993–2007 (2016).
39. A. Banerjee, J. Lee, S. Mitragotri, Intestinal mucoadhesive devices for oral delivery of insulin. *Bioeng. Transl. Med.* **1**, 338–346 (2016).
40. K. Han, J. Nam, J. Xu, X. Sun, X. Huang, O. Animasahun, A. Achreja, J. H. Jeon, B. Pursley, N. Kamada, G. Y. Chen, D. Nagrath, J. J. Moon, Generation of systemic antitumour immunity via the in situ modulation of the gut microbiome by an orally administered inulin gel. *Nat. Biomed. Eng.* **5**, 1377–1388 (2021).

41. A. M. El-Tawil, Trends on gastrointestinal bleeding and mortality: Where are we standing? *World J. Gastroenterol.* **18**, 1154–1158 (2012).
42. Y. Iida, S. Miura, Y. Munemoto, Y. Kasahara, Y. Asada, D. Toya, M. Fujisawa, Endoscopic resection of large colorectal polyps using a clipping method. *Dis. Colon Rectum* **37**, 179–180 (1994).
43. S. Zhang, J. Ermann, M. D. Succi, A. Zhou, M. J. Hamilton, B. Cao, J. R. Korzenik, J. N. Glickman, P. K. Vemula, L. H. Glimcher, G. Traverso, R. Langer, J. M. Karp, An inflammation-targeting hydrogel for local drug delivery in inflammatory bowel disease. *Sci. Transl. Med.* **7**, 300ra128 (2015).
44. K. Nan, V. Feig, B. Ying, J. G. Howarth, Z. Kang, Y. Yang, G. Traverso, Mucosa-interfacing electronics. *Nat. Rev. Mater.* **7**, 908–925 (2022).
45. T.-A. Asoh, A. Kikuchi, Electrophoretic adhesion of stimuli-responsive hydrogels. *Chem. Commun.* **46**, 7793–7795 (2010).
46. B. Ying, R. Z. Chen, R. Zuo, J. Li, X. Liu, An anti-freezing, ambient-stable and highly stretchable ionic skin with strong surface adhesion for wearable sensing and soft robotics. *Adv. Funct. Mater.* **31**, 2104665 (2021).
47. K. Stamatopoulos, C. O'Farrell, M. Simmons, H. Batchelor, In vivo models to evaluate ingestible devices: Present status and current trends. *Adv. Drug Deliv. Rev.* **177**, 113915 (2021).

Acknowledgments: We thank G. Liu, V. Feig, and M. Jimenez from MIT for insightful discussions on the manuscript; Y. Yang, Z. Kang, S. You, J.-G. Rosenboom, A. Kirtane, L. DeRidder, I. Moon, X. Huang, S. Qu, K. Wong, and Koch Institute Swanson Biotechnology Center histology and imaging cores from MIT for the discussion and technical support; and R. Bronson and M. Boucher for help with pathology. **Funding:** This work was funded in part by a grant from Novo Nordisk (to R.L. and G.T.); the Karl van Tassel (1925) Career Development Professorship and the Department of Mechanical Engineering, MIT (to G.T.); a Banting Postdoctoral Fellowship and NSERC Postdoctoral Fellowship (to B.Y.); MIT UROP program (to H.R., S.Q., and K.J.); an ETH Zurich SEMP Scholarship and ZENO KARL SCHINDLER Foundation Master Thesis Grant (to Y.C.); and Ningbo Natural Science Foundation (grant no. 2018A610073, to Q.Z.). **Author contributions:** B.Y. and G.T. designed all the experiments supporting the development of e-GLUE. B.Y., T.K., H.R., S.Q., S.W., K.J., Y.C., G.B., A.L., F.C., J.M., and J.L. fabricated the devices and performed the material, mechanical, and electronic characterization. B.Y., K.N., J.J., A.P., J.K., K.I., N.F., and A.H. performed the in vivo experiments. Q.Z. built the COMSOL numerical models. G.T. and R.L. provided the funding and supervised the project. All authors contributed to the writing of the manuscript. **Competing interests:** G.T. and R.L. report receiving grant funding and consulting fees from Novo Nordisk. Complete details of all relationships for both profit and not-for-profit entities for G.T. are available at the following link: http://www.dropbox.com/sh/szi7vnr4a2ajb56/AABs5N5i0q9AfT1IqIJAE-T5a?dl=0. Complete details for R.L. are available at the following link: http://www.dropbox.com/s/yc3xqb5s8s94v7x/Rev%20Langer%20COI.pdf?dl=0. The other authors declare that they have no competing interests. **Data and materials availability:** All data associated with this study are present in the paper or the Supplementary Materials.

Submitted 1 May 2024
Resubmitted 14 September 2024
Accepted 29 January 2025
Published 26 February 2025
10.1126/scitranslmed.adq1975